

Article

A Near-Infrared Fluorescent Probe for Recognition of Hypochlorite Anions Based on Dicyanoisophorone Skeleton

Chang-Xiang Liu ^{1,†}, Shu-Yuan Xiao ^{1,†}, Xiu-Lin Gong ¹, Xi Zhu ^{2,*}, Ya-Wen Wang ^{1,*} and Yu Peng ¹¹ School of Life Science and Engineering, Southwest Jiaotong University, Chengdu 610031, China² Department of Neurology, The Third People's Hospital of Chengdu, The Affiliated Hospital of Southwest Jiaotong University, Chengdu 610031, China

* Correspondence: zhu61900@163.com (X.Z.); ywwang@swjtu.edu.cn (Y.-W.W.)

† These authors contributed equally to this work.

Abstract: A novel near-infrared (NIR) fluorescent probe (SWJT-9) was designed and synthesized for the detection of hypochlorite anion (ClO⁻) using a diaminomaleonitrile group as the recognition site. SWJT-9 had large Stokes shift (237 nm) and showed an excellent NIR fluorescence response to ClO⁻ with the color change under the visible light. It showed a low detection limit (24.7 nM), high selectivity, and rapid detection (within 2 min) for ClO⁻. The new detection mechanism of SWJT-9 on ClO⁻ was confirmed by ¹H NMR, MS spectrum, and the density functional theory (DFT) calculations. In addition, the probe was successfully used to detect ClO⁻ in HeLa cells.

Keywords: fluorescence; hypochlorite anion (ClO⁻); near-infrared probe; chemodosimeter

1. Introduction

Neutrophils, known as polymorphonuclear cells, are the largest number of white blood cells in the body [1–3]. They are the main immune cells that protect the body from microbial infection and eliminate pathogens [4]. In neutrophils, hydrogen peroxide (H₂O₂) reacts with chloride ions to generate hypochlorite anions [5–7] under the catalysis of myeloperoxidase. Hypochlorite anions plays a very important role in the human body [8,9]. However, excessive hypochlorite anion in the body will oxidize biological molecules, such as protein, cholesterol, DNA, and RNA in living cells, which will lead to cardiovascular disease, inflammatory disease, cancer, and so on [10–15]. Therefore, it is necessary to monitor hypochlorite anions in vitro and in vivo.

At present, many analytical methods have been applied to the detection of hypochlorite anions, such as colorimetry, luminescence, electrochemistry, and chromatography [16–18]. In addition, the fluorescence probing method was paid more attention as an excellent detection tool, which has realized the detection of many active species [19–23]. Fluorescence probes for the detection of hypochlorite anions have been reported continuously in recent years [24–46]. Among them, some chemodosimeters using a diaminomaleonitrile group as the reaction site were used to detect hypochlorite anions, which had many advantages, such as specific recognition, high selectivity, and fast response. However, most chemodosimeters for the hypochlorite anion could hardly achieve near-infrared fluorescence emission and did not have a large Stokes shift (Table S1) [34–46]. It is well known that NIR fluorescent probes with a large Stokes shift have more advantages due to good applications in biological systems [47]. Therefore, it is necessary to design a near-infrared fluorescent probe with a large Stokes shift for the detection of hypochlorite anions with high selectivity and rapid response.

In connection with our previous work [26,48,49], herein, we reported a novel chemodosimeter (SWJT-9), which had a large Stokes shift and emitted near-infrared fluorescence due to using a dicyanoisophorone skeleton. It can specifically recognize a hypochlorite



Citation: Liu, C.-X.; Xiao, S.-Y.; Gong, X.-L.; Zhu, X.; Wang, Y.-W.; Peng, Y. A Near-Infrared Fluorescent Probe for Recognition of Hypochlorite Anions Based on Dicyanoisophorone Skeleton. *Molecules* **2023**, *28*, 402. <https://doi.org/10.3390/molecules28010402>

Academic Editors: Yuanwei Zhang and Ling Huang

Received: 27 November 2022

Revised: 23 December 2022

Accepted: 24 December 2022

Published: 3 January 2023



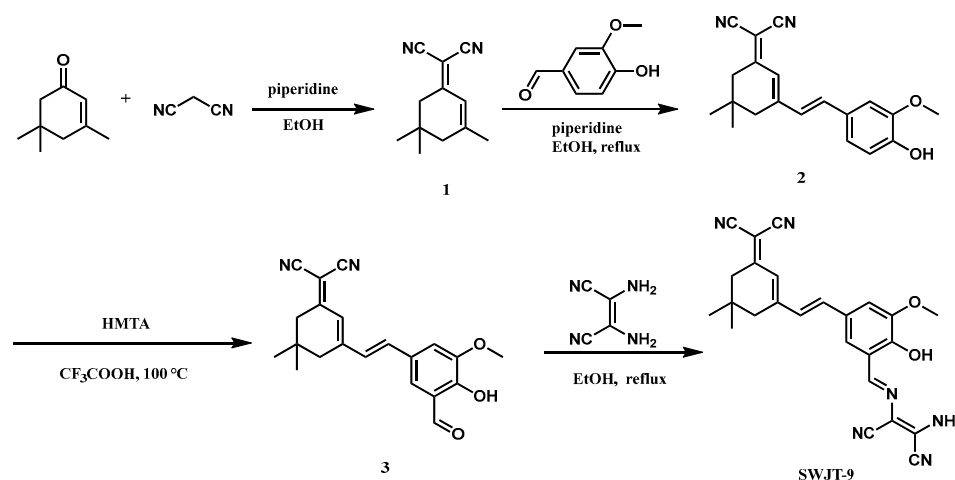
Copyright: © 2023 by the authors. Licensee MDPI, Basel, Switzerland. This article is an open access article distributed under the terms and conditions of the Creative Commons Attribution (CC BY) license (<https://creativecommons.org/licenses/by/4.0/>).

anion based on the inhibition of C=N rotational isomerization [50]. Moreover, **SWJT-9** was successfully applied to HeLa cell imaging.

2. Results and Discussion

2.1. Design **SWJT-9**

Through the Duff reaction, an aldehyde group was generated at the ortho position of the hydroxyl group in a dicyanoisophorone skeleton. The diaminomaleonitrile group was then used as the recognition group [36,51] to obtain the probe **SWJT-9** (Scheme 1). The structure of **SWJT-9** was confirmed by NMR and MS (Figures S1–S3, Supplementary Materials). The fluorescence of **SWJT-9** would reduce by the rotational isomerization of the C=N double bond [52]. After the addition of hypochlorite anions, a reaction between **SWJT-9** and ClO^- would occur to obtain compound **3**, which had no C=N bond; therefore, the fluorescence would be enhanced [53–55].



Scheme 1. Synthesis of **SWJT-9**.

2.2. Photoproperties of Probe

In order to study the effect of organic solvents on the probe, methanol, ethanol, acetonitrile, DMSO, and DMF were used (Figure S4, Supplementary Materials). The effect of the buffer solution and pH on the probe were also studied (Figure S5, Supplementary Materials). According to these results, and considering the solubility of the probe, the solution of ethanol and PBS (9/1, *v/v*) at pH 7.4 was selected as the test condition.

As shown in Figure 1a, the UV–Vis absorption spectrum of **SWJT-9** showed an obvious absorption band centered at 430 nm. After the addition of ClO^- to the solution, the absorbance red-shifted to about 550 nm. The color of the solution changed from yellow to pink (Figure 1a, inset). These results suggested that a reaction might occur between **SWJT-9** and ClO^- . In the fluorescence spectrum, **SWJT-9** showed weak emission at about 667 nm ($\Phi = 0.018$) under excitation at 550 nm (Figure 1b). After the addition of ClO^- , the fluorescence increased ($\Phi = 0.113$) [56], and the fluorescence color of the solution was observed from red to deep red (Figure 1b, inset). These results indicated that **SWJT-9** could detect hypochlorite anions by colorimetric and fluorescence turn-on responses. The fluorescence titration experiments were then conducted. As shown in Figure 1c, the fluorescence intensity enhanced with the increase of the ClO^- concentration, indicating that **SWJT-9** was a turn-on fluorescence probe. The detection limit was calculated as 24.7 nM (Figure S6, Supplementary Materials), which was far lower than the concentration of hypochlorite anions produced by cells [57].

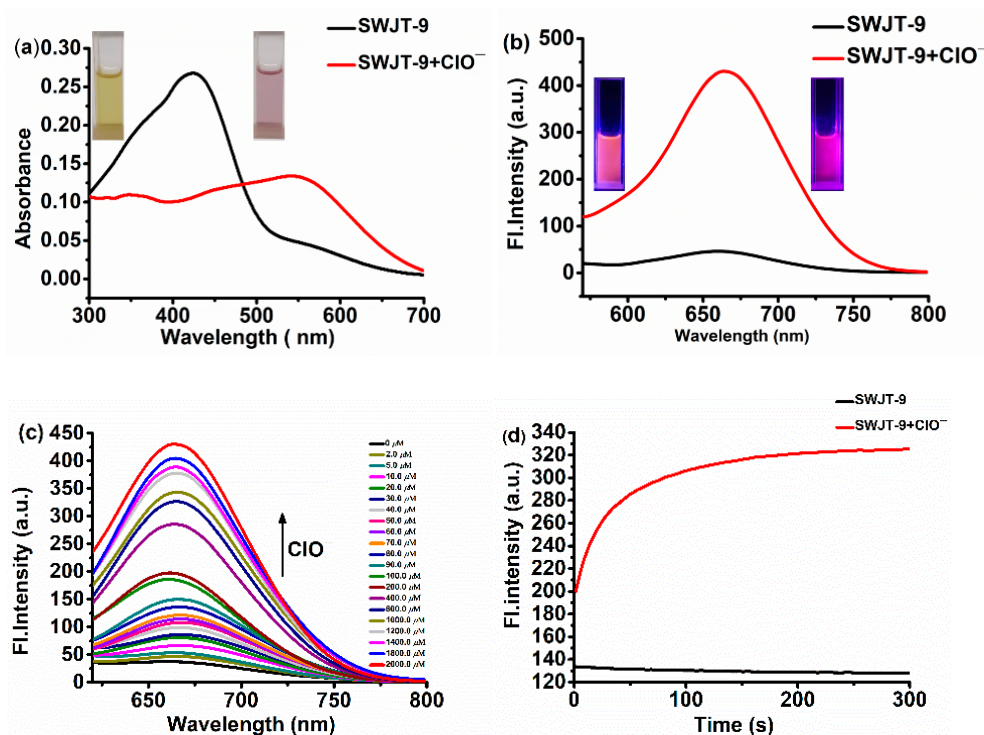


Figure 1. (a) Absorption spectra of SWJT-9 (10.0 μM) and SWJT-9 + ClO⁻ (2.0 mM) in EtOH-PBS (9/1, v/v, pH 7.4) buffer solution. Inset: images of SWJT-9 (left) and SWJT-9 after adding ClO⁻ (right) under visible light. (b) Fluorescence spectra of SWJT-9 (10.0 μM) and SWJT-9 + ClO⁻ (2.0 mM) in EtOH-PBS (9/1, v/v, pH 7.4) buffer solution ($\lambda_{\text{ex}} = 550 \text{ nm}$). Inset: images of SWJT-9 (left) and SWJT-9 + ClO⁻ (right) after adding ClO⁻ under UV light. (c) Fluorescence titrations of SWJT-9 (10.0 μM) with different concentrations of ClO⁻ (0–2000.0 μM) ($\lambda_{\text{ex}} = 550 \text{ nm}$). (d) The fluorescence intensity of the SWJT-9 (10.0 μM) and ClO⁻ (2.0 mM) probes increased with time ($\lambda_{\text{em}} = 667 \text{ nm}$).

In addition, it is well known that the reaction time is an important parameter for examining intracellular hypochlorite anions [28]. The shorter the time, the better the recognition. As shown in Figure 1d, the fluorescence intensity tends to equilibrate within two minutes. These results showed that this probe has high sensitivity to hypochlorite anions. Moreover, the constant (k_{obs}) of the pseudo-first-order reaction was calculated to be 0.03041 s^{-1} , and the $t_{1/2}$ was 23 s (Figure S7, Supplementary Materials).

2.3. Competition Experiments

As shown in Figure 2, when active oxygen species or other anions were added to the solution of SWJT-9, the fluorescence intensity was still weak. The fluorescence intensity at 667 nm significantly enhanced when ClO⁻ was added to the above solution. These results indicated that the presence of other reactive oxygen species or anions would not interfere with the recognition of ClO⁻ by SWJT-9. The probe had a good anti-interference property and potential application in biological environments.

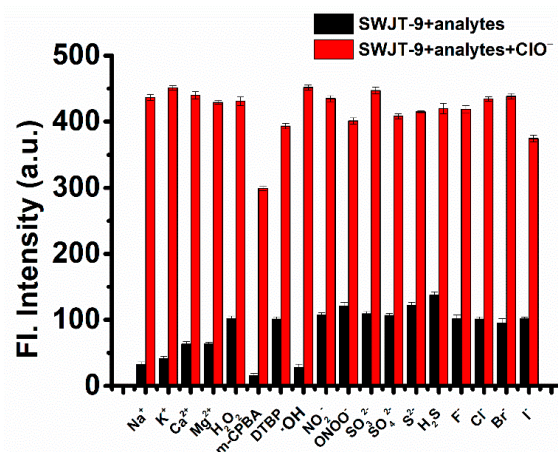


Figure 2. Fluorescence response of probe **SWJT-9** (10.0 μM) toward ClO^- (2.0 mM) and various analytes (2.0 mM) in the EtOH/PBS buffer solution (9:1, v/v , pH 7.4). Black bar: **SWJT-9** + various analytes; red bar: **SWJT-9** + various analytes + ClO^- . $\lambda_{\text{em}} = 667 \text{ nm}$.

2.4. Response Mechanism

In order to verify the possible reaction mechanism of **SWJT-9** and ClO^- , ^1H NMR titration (Figure 3) and MS spectrum (Figure S8, Supplementary Materials) were used. As shown in Figure 3, the proton signal of the C=N bond (H_a) appeared at 8.5 ppm. When ClO^- was added, the peak (H_a) disappeared gradually while a new proton (H_b) appeared. Compared with two spectrum (**SWJT-9** + ClO^- and compound **3**), they were basically the same, which indicated **3** was the product from a reaction of **SWJT-9** and ClO^- . In addition, as shown in Figure S8 (Supplementary Materials), the peak at m/z 349.3 of **SWJT-9** + ClO^- corresponds to **3**.

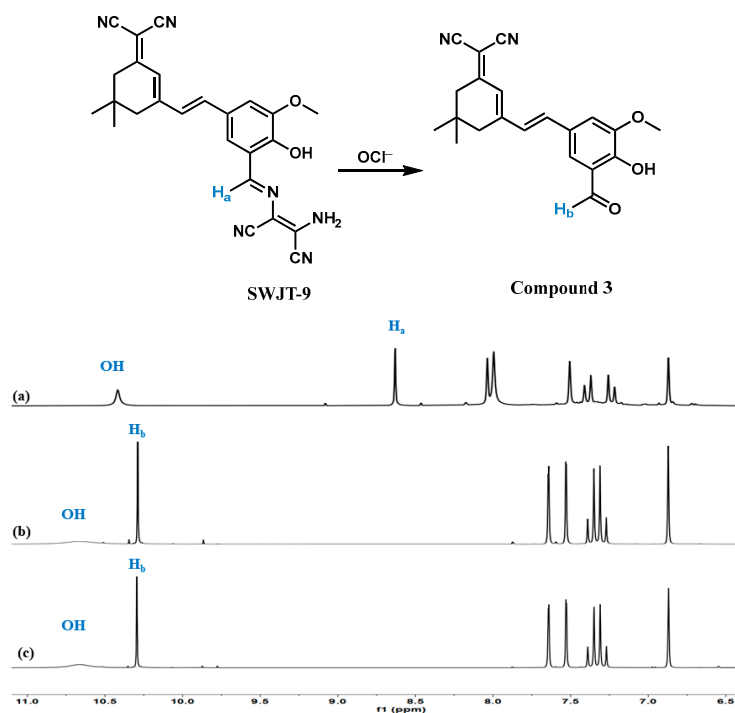


Figure 3. Partial ^1H NMR spectra of (a) **SWJT-9**, (b) **SWJT-9** + ClO^- , and (c) compound **3** in $\text{DMSO}-d_6$ (400 MHz).

2.5. DFT Calculations

In order to investigate the relationship between the probe and the spectral changes, density functional theory (DFT, B3LYP/6-311G, Gaussian 09) calculations were performed [58]. As shown in Figure 4, the HOMO electron density of **SWJT-9** was distributed on the dicyanoisophorone skeleton and diaminomaleonitrile group. However, for the LUMO level, the electron density was only located on the dicyanoisophorone skeleton, which meant that C=N isomerization occurred to lead to the weak fluorescence of **SWJT-9** [59]. At the HOMO and LUMO levels, the electrons of compound **3** were all mainly distributed in the whole dicyanoisophorone group, indicating that compound **3** had a strong fluorescence emission. These results suggested that **SWJT-9** could be considered as a turn-on probe for ClO^- .

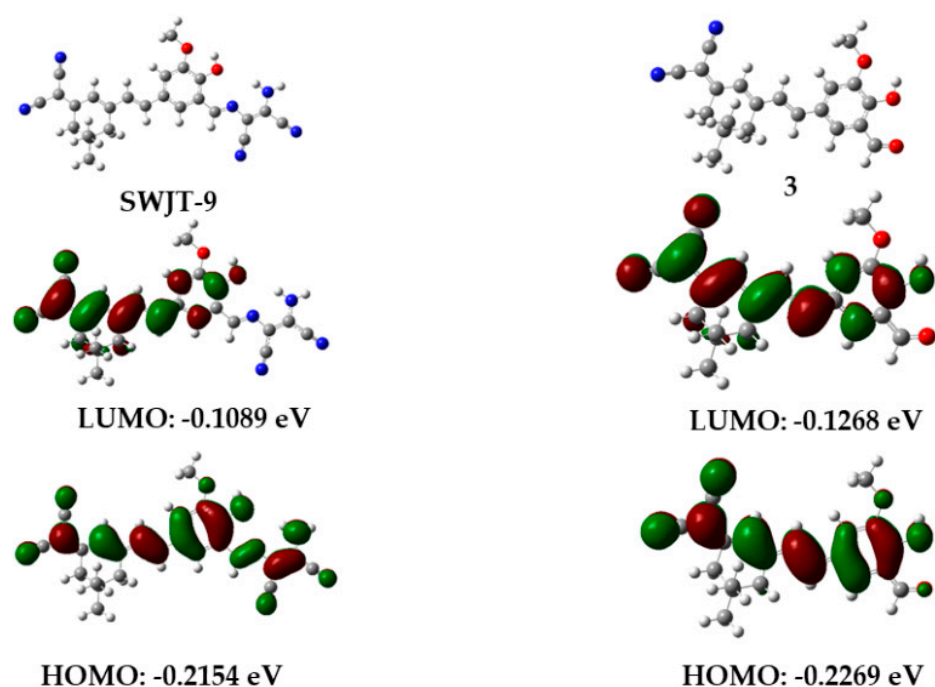


Figure 4. Optimized structures and molecular orbital plots of **SWJT-9** and compound **3**.

2.6. Cytotoxicity of **SWJT-9** and Its Imaging in HeLa Cells

In order to further prove the excellent performance of the near-infrared fluorescence of **SWJT-9**, HeLa cells were used (Figure 5) to study bioimaging. First, HeLa cells were incubated with **SWJT-9** (10.0 μM) for 30 min. As shown in Figure 5b, the fluorescence of **SWJT-9** was very weak in the red channel. In the other group, **SWJT-9** and HeLa cells were incubated at 37 $^{\circ}\text{C}$ for 30 min and then incubated with ClO^- for another 20 min. The fluorescence in the red channel improved obviously. These results indicated that **SWJT-9** has good cell membrane transparency and can detect ClO^- in HeLa cells. In addition, the CCK test results showed that **SWJT-9** did not produce significant cytotoxicity in HeLa cells (Figure 6).

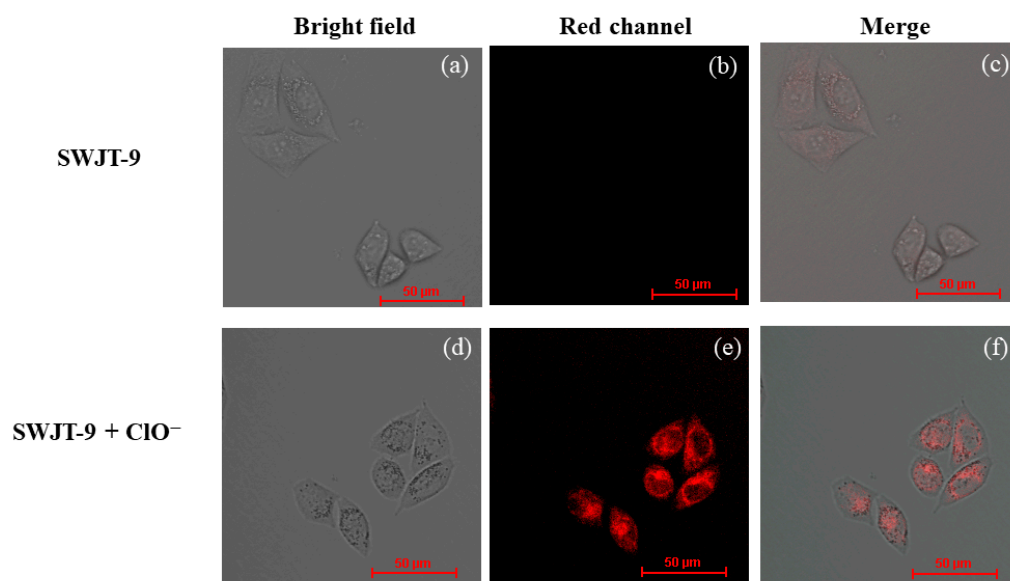


Figure 5. Fluorescence images of HeLa cells. (a–c) **SWJT-9** (10.0 μM) imaged with HeLa cells for 30 min; (d–f) HeLa cells incubated with **SWJT-9** (10.0 μM) for 30 min, then incubated with ClO^- (200.0 μM) for another 20 min ($\lambda_{\text{ex}} = 561 \text{ nm}$).

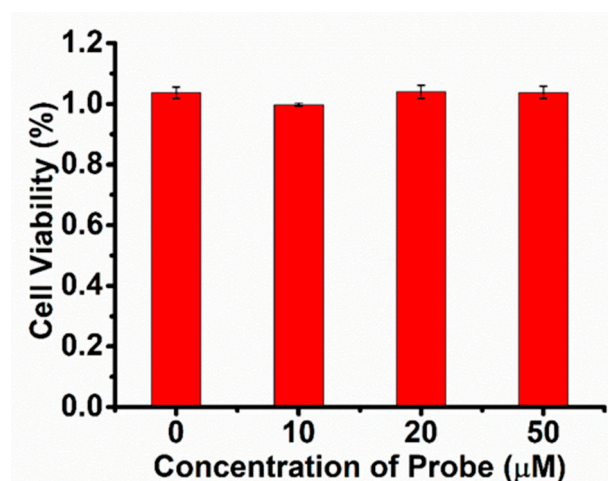


Figure 6. Toxicity of probe concentration in HeLa cells.

3. Materials and Methods

3.1. Materials and Reagents

The materials, reagents, and detection methods are described in the Supplementary Materials.

3.2. Synthesis of Probe **SWJT-9**

Compound **1** and compound **2** were prepared according to the previously reported literature [60].

Compound **2** (5.01 g, 15.61 mmol) and hexamethylenetetramine (4.16 g, 29.65 mmol) were dissolved in trifluoroacetic acid (20 mL), heated to 100 $^{\circ}\text{C}$, and reacted for 8 h. The mixture solution was cooled to room temperature and extracted with CH_2Cl_2 ($2 \times 150 \text{ mL}$). Finally, the collected organic layers were concentrated and purified by column chromatography (petroleum ether:ethyl acetate = 4:1) on silica gel to obtain the known compound **3** [49] (1.80 g, 33.1%).

Compound **3** (90.10 mg, 0.26 mmol) and diaminomaleonitrile (32.01 mg, 0.30 mmol) were added to ethanol (10 mL). Then, the mixture was heated at 80 $^{\circ}\text{C}$ for two hours

and then filtered with suction. After washing with ethanol, **SWJT-9** can be obtained as a solid. Yield: 45.0 %. ^1H NMR (400 MHz, $\text{DMSO-}d_6$): δ = 10.34 (s, 1H), 8.58 (s, 1H), 8.0 (s, 1H), 7.95 (s, 1H), 7.47 (s, 1H), 7.37 (d, J = 16.0 Hz, 1H), 7.22 (d, J = 16.0 Hz, 1H), 6.84 (s, 1H), 3.93 (s, 3H), 2.62 (s, 2H), 2.53 (s, 2H), 1.03 (s, 6H) ppm. ^{13}C NMR (100 MHz, $\text{DMSO-}d_6$): δ = 170.7, 156.6, 151.8, 150.0, 148.9, 138.3, 128.0, 127.9, 126.9, 122.3, 122.3, 121.4, 114.9, 114.5, 114.3, 113.7, 113.2, 103.8, 75.9, 56.7, 42.8, 38.8, 32.2, 27.9 (2C) ppm. ESI-MS: m/z 439.1 $[\text{M} + \text{H}]^+$.

4. Conclusions

In conclusion, a near-infrared fluorescent probe **SWJT-9** for ClO^- detection was developed. It exhibited a large Stokes shift (237 nm), high selectivity, good sensitivity, and fast response. An obvious color change was observed by the naked eye under visible light or ultraviolet light. **SWJT-9** was a new near-infrared fluorescent probe using diaminomaleonitrile as the recognition group, and it can be successfully used in cells, indicating its potential use in biological analyses. This work could provide some inspiration for future research of near-infrared fluorescence probes.

Supplementary Materials: The following are available online at <https://www.mdpi.com/article/10.3390/molecules28010402/s1>: Copies of ^1H , ^{13}C NMR, ESI-MS spectra, spectral data, and other materials [61].

Author Contributions: Y.-W.W. conceived and designed the experiments; C.-X.L. and S.-Y.X. performed the experiments; C.-X.L., S.-Y.X., X.-L.G., X.Z., Y.-W.W. and Y.P. analyzed the data; and C.-X.L., X.Z., Y.-W.W. and Y.P. wrote the paper. All authors have read and agreed to the published version of the manuscript.

Funding: This work was supported by the National Natural Science Foundation of China (No. 21572091). We also thank the Science and Technology Department of Sichuan Province (2020JDR0021) and Key Research Project of Sichuan Province Science and Technology Plan (2020YFS0489).

Institutional Review Board Statement: Not applicable.

Informed Consent Statement: Not applicable.

Data Availability Statement: Not applicable.

Acknowledgments: We would like to thank the Analytical and Testing Center of Southwest Jiaotong University for the NMR and laser confocal microscope test.

Conflicts of Interest: The authors declare no conflict of interest.

References

1. Xu, R.; Huang, H.; Zhang, Z.; Wang, F.-S. The role of neutrophils in the development of liver diseases. *Cell. Mol. Immunol.* **2014**, *11*, 224–231. [[CrossRef](#)] [[PubMed](#)]
2. Li, A.; Grönlund, E.; Brattsand, G. Automated white blood cell counts in cerebrospinal fluid using the body fluid mode on the platform Sysmex XE-5000. *Scand. J. Clin. Lab. Investig.* **2014**, *74*, 673–680. [[CrossRef](#)] [[PubMed](#)]
3. Leliefeld, P.H.C.; Wessels, C.M.; Leenen, L.P.H.; Koenderman, L.; Pillay, J. The role of neutrophils in immune dysfunction during severe inflammation. *Crit. Care* **2016**, *20*, 73. [[CrossRef](#)] [[PubMed](#)]
4. Lippolis, J.D. Immunological signaling networks: Integrating the body's immune response. *J. Anim. Sci.* **2008**, *86*, 53–63. [[CrossRef](#)] [[PubMed](#)]
5. Shao, B.H.; Belaaouaj, A.; Verlinde, C.M.L.J.; Fu, X.J.; Heinecke, J.W. Methionine sulfoxide and proteolytic cleavage contribute to the inactivation of cathepsin G by hypochlorous acid: An oxidative mechanism for regulation of serine proteinases by myeloperoxidase. *J. Biol. Chem.* **2005**, *280*, 29311–29321. [[CrossRef](#)] [[PubMed](#)]
6. Winterbourn, C.C. Biological reactivity and biomarkers of the neutrophil oxidant, hypochlorous acid. *Toxicology* **2002**, *181*, 223–227. [[CrossRef](#)]
7. Miyamoto, G.; Zahid, N.; Uetrecht, J.P. Oxidation of Diclofenac to Reactive Intermediates by Neutrophils, Myeloperoxidase, and Hypochlorous Acid. *Chem. Res. Toxicol.* **1997**, *10*, 414–419. [[CrossRef](#)]
8. Seminko, V.; Maksimchuk, P.; Grygorova, G.; Avrunin, O.; Semenets, V.; Klochkov, V.; Malyukin, Y. Catalytic Decomposition of Hypochlorite Anions by Ceria Nanoparticles Visualized by Spectroscopic Techniques. *J. Phys. Chem. C* **2019**, *123*, 20675–20681. [[CrossRef](#)]

9. Stanley, N.R.; Pattison, D.I.; Hawkins, C.L. Ability of Hypochlorous Acid and N-Chloramines to Chlorinate DNA and Its Constituents. *Chem. Res. Toxicol.* **2010**, *23*, 1293–1302. [[CrossRef](#)]
10. Stéliana, G.; Carole, R.; Catherine, V.; Marianne, Z.; Cottin, Y.; Luc, R. Antioxidant properties of an endogenous thiol: Al-pha-lipoic acid, useful in the prevention of cardiovascular diseases. *J. Cardiovasc. Pharm.* **2009**, *54*, 391–398.
11. Pattison, D.; Davies, M.J. Kinetic analysis of the role of histidine chloramines in hypochlorous acid mediated protein oxidation. *Biochemistry* **2005**, *44*, 7378–7387. [[CrossRef](#)] [[PubMed](#)]
12. Aiken, M.L.; Painter, R.G.; Zhou, Y.; Wang, G. Chloride transport in functionally active phagosomes isolated from Human neutrophils. *Free. Radic. Biol. Med.* **2012**, *53*, 2308–2317. [[CrossRef](#)] [[PubMed](#)]
13. Pattison, D.; Davies, M.J. Absolute rate constants for the reaction of hypochlorous acid with protein side chains and peptide bonds. *Chem. Res. Toxicol.* **2001**, *14*, 1453–1464. [[CrossRef](#)] [[PubMed](#)]
14. Savenkova, M.; Mueller, D.; Heinecke, J. Tyrosyl radical generated by myeloperoxidase is a physiological catalyst for the initiation of lipid peroxidation in low density lipoprotein. *J. Biol. Chem.* **1994**, *269*, 20394–20400. [[CrossRef](#)] [[PubMed](#)]
15. Wu, S.M.; Pizzo, S.V. α 2-Macroglobulin from Rheumatoid Arthritis Synovial Fluid: Functional Analysis Defines a Role for Oxidation in Inflammation. *Arch. Biochem. Biophys.* **2001**, *391*, 119–126. [[CrossRef](#)]
16. Claver, J.B.; Valencia Miron, M.C.; Capit'an-Vallvey, L.F. Determination of hypochlorite in water using a chemiluminescent test strip. *Anal. Chim. Acta.* **2004**, *522*, 267–273. [[CrossRef](#)]
17. Chen, P.; Wei, W.-Z.; Yao, S.-Z. Different valency chlorine species analysis by non-suppressed ion-chromatography with double cell quartz crystal detector. *Talanta* **1999**, *49*, 571–576. [[CrossRef](#)]
18. Hallaj, T.; Amjadi, M.; Manzoori, J.; Shokri, R. Chemiluminescence reaction of glucose-derived graphene quantumdots with hypochlorite, and its application to the determination of free chlorine. *Microchim. Acta.* **2015**, *182*, 789–796. [[CrossRef](#)]
19. Dikalov, S.I.; Harrison, D.G. Methods for Detection of Mitochondrial and Cellular Reactive Oxygen Species. *Antioxid. Redox Signal.* **2014**, *20*, 372–382. [[CrossRef](#)]
20. Qu, Z.; Ding, J.; Zhao, M.; Li, P. Development of a selenide-based fluorescent probe for imaging hypochlorous acid in lyso-somes. *J. Photoch. Photobio. A* **2015**, *299*, 1–8. [[CrossRef](#)]
21. Wu, L.; Sedgwick, A.C.; Sun, X.; Bull, S.D.; He, X.-P.; James, T.D. Reaction-Based Fluorescent Probes for the Detection and Imaging of Reactive Oxygen, Nitrogen, and Sulfur Species. *Accounts Chem. Res.* **2019**, *52*, 2582–2597. [[CrossRef](#)] [[PubMed](#)]
22. Ren, T.; Wang, Z.; Xiang, Z.; Lu, P.; Lai, H.; Yuan, L.; Zhang, X.; Tan, W. A General Strategy for Development of Activatable NIR-II Fluorescent Probes for In Vivo High-Contrast Bioimaging. *Angew. Chem. Int. Ed.* **2020**, *60*, 800–805. [[CrossRef](#)] [[PubMed](#)]
23. Wei, Y.; Liu, Y.; He, Y.; Wang, Y. Mitochondria and lysosome-targetable fluorescent probes for hydrogen peroxide. *J. Mater. Chem. B* **2021**, *9*, 908–920. [[CrossRef](#)] [[PubMed](#)]
24. Pang, Q.; Li, T.; Yin, C.; Ma, K.; Huo, F. Comparing the abundance of HClO in cancer/normal cells and visualizing in vivo using a mitochondria-targeted ultra-fast fluorescent probe. *Analyst* **2021**, *146*, 3361–3367. [[CrossRef](#)]
25. Wu, P.; Zhu, Y.; Chen, L.; Tian, Y.; Xiong, H. A Fast-Responsive OFF–ON Near-Infrared-II Fluorescent Probe for In Vivo Detection of Hypochlorous Acid in Rheumatoid Arthritis. *Anal. Chem.* **2021**, *93*, 13014–13021. [[CrossRef](#)] [[PubMed](#)]
26. Xu, H.; Wu, S.-L.; Song-Ling, W.; Lu, Y.; Xiao, J.; Wang, Y.-W.; Peng, Y. A NIR fluorescent probe for rapid turn-on detection and bioimaging of hypochlorite anion. *Sens. Actuators B Chem.* **2021**, *346*, 130484. [[CrossRef](#)]
27. Duan, C.; Won, M.; Verwilt, P.; Xu, J.; Kim, H.S.; Zeng, L.; Kim, J.S. In Vivo Imaging of Endogenously Produced HClO in Zebrafish and Mice Using a Bright, Photostable Ratiometric Fluorescent Probe. *Anal. Chem.* **2019**, *91*, 4172–4178. [[CrossRef](#)]
28. Gao, W.; Ma, Y.; Liu, Y.; Ma, S.; Lin, W. Observation of endogenous HClO in living mice with inflammation, tissue injury and bacterial infection by a near-infrared fluorescent probe. *Sens. Actuators B Chem.* **2021**, *327*, 128884. [[CrossRef](#)]
29. Cheng, G.; Fan, J.; Sun, W.; Sui, K.; Jin, X.; Wang, J.; Peng, X. A highly specific BODIPY-based probe localized in mitochondria for HClO imaging. *Analyst* **2013**, *138*, 6091–6096. [[CrossRef](#)]
30. Wang, L.; Ding, H.; Ran, X.; Tang, H.; Cao, D. Recent progress on reaction-based BODIPY probes for anion detection. *Dye. Pigment.* **2020**, *172*, 107857. [[CrossRef](#)]
31. Wang, L.; Liu, J.; Zhang, H.; Guo, W. Discrimination between cancerous and normal cells/tissues enabled by a near-infrared fluorescent HClO probe. *Sens. Actuators B Chem.* **2021**, *334*, 129602. [[CrossRef](#)]
32. Li, H.; Kim, H.; Han, J.; Nguyen, V.N.; Peng, X.; Yoon, J. Activity-based smart AIEgens for detection, bioimaging, and therapeutics: Recent progress and outlook. *Aggregate* **2021**, *2*, 51. [[CrossRef](#)]
33. Hu, Q.; Qin, C.; Huang, L.; Wang, H.; Liu, Q.; Zeng, L. Selective visualization of hypochlorite and its fluctuation in cancer cells by a mitochondria-targeting ratiometric fluorescent probe. *Dye. Pigment.* **2018**, *149*, 253–260. [[CrossRef](#)]
34. Feng, Y.; Li, S.Q.; Li, D.X.; Wang, Q.; Ning, P.; Chen, M.; Tian, X.H. Rational design of a diaminomaleonitrile-based mitochondria—Targeted two-photon fluorescent probe for hypochlorite in vivo: Solvent-independent and high selectivity over Cu²⁺. *Sens. Actuators B Chem.* **2018**, *254*, 282–290. [[CrossRef](#)]
35. Dou, K.; Fu, Q.; Chen, G.; Yu, F.B.; Liu, Y.X.; Cao, Z.P.; Li, G.L.; Zhao, X.N.; Xia, L.; Chen, L.X.; et al. A novel dual-ratiometric-response fluorescent probe for SO₂/ClO[−] detection in cells and in vivo and its application in exploring the dichotomous role of SO₂ under the ClO[−] induced oxidative stress. *Biomaterials* **2017**, *133*, 82–93. [[CrossRef](#)]
36. Ning, Y.; Cui, J.; Lu, Y.; Wang, X.; Xiao, C.; Wu, S.; Li, J.; Zhang, Y. De novo design and synthesis of a novel colorimetric fluorescent probe based on naphthalenone scaffold for selective detection of hypochlorite and its application in living cells. *Sens. Actuators B Chem.* **2018**, *269*, 322–330. [[CrossRef](#)]

37. Malkondu, S.; Erdemir, S.; Karakurt, S. Red and blue emitting fluorescent probe for cyanide and hypochlorite ions: Biological sensing and environmental analysis. *Dye. Pigment.* **2020**, *174*, 108019. [[CrossRef](#)]
38. Zhang, Y.; Ma, L.; Tang, C.; Pan, S.; Shi, D.; Wang, S.; Li, M.; Guo, Y. A highly sensitive and rapidly responding fluorescent probe based on a rhodol fluorophore for imaging endogenous hypochlorite in living mice. *J. Mater. Chem. B* **2018**, *6*, 725. [[CrossRef](#)]
39. Wang, Z.; Zhang, Y.; Song, J.; Li, M.; Yang, Y.; Gu, W.; Xu, X.; Xu, H.; Wang, S. A highly specific and sensitive turn-on fluorescence probe for hypochlorite detection based on anthracene fluorophore and its bioimaging applications. *Dye. Pigment.* **2018**, *161*, 172–181. [[CrossRef](#)]
40. Tang, X.; Zhu, X.; Liu, R.J.; Tang, Y. A novel ratiometric and colorimetric fluorescent probe for hypochlorite based on cyanobiphenyl and its applications. *Spectrochim. Acta Part A Mol. Biomol. Spectrosc.* **2019**, *219*, 576–581. [[CrossRef](#)]
41. Zhao, X.J.; Jiang, Y.R.; Chen, Y.X.; Yang, B.Q.; Li, Y.T.; Liu, Z.H.; Liu, C. A new “off-on” NIR fluorescence probe for determination and bio-imaging of mitochondrial hypochlorite in living cells and zebrafish. *Spectrochim. Acta. A* **2019**, *219*, 509–516. [[CrossRef](#)] [[PubMed](#)]
42. Cheng, W.S.; Ren, C.P.; Liu, S.; Jiang, W.S.; Zhu, X.N.; Jia, W.X.; Chen, J.B.; Liu, Z.B. A highly selective A- π -A “turn-on” fluorescent probe for hypochlorite in tap water. *New J. Chem.* **2022**, *46*, 18010–18017. [[CrossRef](#)]
43. Zhang, X.W.; Zhang, F.; Chai, J.; Yang, B.S.; Liu, B. A TICT + AIE based fluorescent probe for ultrafast response of hypochlorite in living cells and mouse. *Spectrochim. Acta. A* **2021**, *256*, 119735. [[CrossRef](#)] [[PubMed](#)]
44. Xu, C.; Wu, T.; Duan, L.; Zhou, Y.; Zhou, Y. Rational Design of ICT-Based Fluorescent Probe with AIE and NIR Properties for Hypochlorite Determination. *J. Electrochem. Soc.* **2022**, *169*, 017514. [[CrossRef](#)]
45. Li, M.; Du, F.; Xue, P.; Tan, X.; Liu, S.; Zhou, Y.; Chen, J.; Bai, L. An AIE fluorescent probe with a naphthalimide derivative and its application for detection of hypochlorite and imaging inside living cells. *Spectrochim. Acta A* **2020**, *227*, 117760. [[CrossRef](#)]
46. Jiang, Y.; Wu, S.; Jin, C.; Wang, B.; Shen, J. Novel diaminomaleonitrile-based fluorescent probe for ratiometric detection and bioimaging of hypochlorite. *Sens. Actuators B Chem.* **2018**, *265*, 365–370. [[CrossRef](#)]
47. Zhao, J.; Ma, T.; Chang, B.; Fang, J. Recent Progress on NIR Fluorescent Probes for Enzymes. *Molecules* **2022**, *27*, 5922. [[CrossRef](#)]
48. Feng, Y.-A.; Xu, H.; Zhou, Y.; Wang, B.-J.; Xiao, J.; Wang, Y.-W.; Peng, Y. Ratiometric detection and bioimaging of endogenous alkaline phosphatase by a NIR fluorescence probe. *Sens. Actuators B Chem.* **2022**, *358*, 131505. [[CrossRef](#)]
49. Xu, H.; Zhang, C.; Zhang, Y.-Q.; Suo, S.-N.; Wang, Y.-W.; Peng, Y. A red-NIR fluorescence probe for rapid and visual detection of acrolein. *Chem. Commun.* **2022**, *58*, 10080–10083. [[CrossRef](#)]
50. Yudhistira, T.; Mulay, S.V.; Kim, Y.; Halle, M.B.; Churchill, D.G. Imaging of hypochlorous acid by fluorescence and applications in biological systems. *Chem. Asian. J.* **2019**, *14*, 3048–3084. [[CrossRef](#)]
51. Hwang, S.M.; Yun, D.; Kim, C. An Imidazo[1,5- α]Pyridine-Based Fluorometric Chemodosimeter for the Highly Selective Detection of Hypochlorite in Aqueous Media. *J. Fluoresc.* **2019**, *29*, 451–459. [[CrossRef](#)] [[PubMed](#)]
52. Shi, Y.; Huo, F.; Yin, C. Malononitrile as the ‘double-edged sword’ of passivation-activation regulating two ICT to highly sensitive and accurate ratiometric fluorescent detection for hypochlorous acid in biological system. *Sens. Actuators B Chem.* **2020**, *325*, 128793. [[CrossRef](#)] [[PubMed](#)]
53. He, L.; Xiong, H.; Wang, B.; Zhang, Y.; Wang, J.; Zhang, H.; Li, H.; Yang, Z.; Song, X. Rational design of a two-photon ratiometric fluorescent probe for hypochlorous acid with a large Stokes shift. *Anal. Chem.* **2020**, *92*, 11029–11034. [[CrossRef](#)] [[PubMed](#)]
54. Cheng, G.; Fan, J.; Sun, W.; Cao, J.; Hu, C.; Peng, X. A near-infrared fluorescent probe for selective detection of HClO based on Se-sensitized aggregation of heptamethine cyanine dye. *Chem. Commun.* **2013**, *50*, 1018–1020. [[CrossRef](#)] [[PubMed](#)]
55. Liu, H.B.; Xu, H.; Guo, X.; Xiao, J.; Cai, Z.H.; Wang, Y.W.; Peng, Y. A novel near-infrared fluorescent probe based on iso-phorone for the bioassay of endogenous cysteine. *Org. Biomol. Chem.* **2021**, *19*, 873–877. [[CrossRef](#)]
56. Sun, Q.; Yang, S.; Wu, L.; Dong, Q.; Yang, W.; Yang, G. Detection of intracellular selenol-containing molecules using a fluorescent probe with near-zero background signal. *Anal. Chem.* **2016**, *88*, 6084–6091. [[CrossRef](#)]
57. Lapenna, D.; Cuccurullo, F. Hypochlorous acid and its pharmacological antagonism: An update picture. *Gen. Pharmacol.* **1996**, *27*, 1145–1147. [[CrossRef](#)]
58. Wang, B.J.; Liu, R.J.; Fang, J.G.; Wang, Y.W.; Peng, Y. A water-soluble dual-site fluorescent probe for the rapid detection of cysteine with high sensitivity and specificity. *Chem. Commun.* **2019**, *55*, 11762–11765. [[CrossRef](#)]
59. Wu, J.; Liu, W.; Ge, J.; Zhang, H.; Wang, P. New sensing mechanisms for design of fluorescent chemosensors emerging in recent years. *Chem. Soc. Rev.* **2011**, *40*, 3483–3495. [[CrossRef](#)]
60. Qian, M.; Xia, J.; Zhang, L.; Chen, Q.; Guo, J.; Cui, H.; Kafuti, Y.S.; Wang, J.; Peng, X. Rationally modifying the dicyanoisophorone fluorophore for sensing cysteine in living cells and mice. *Sens. Actuators B Chem.* **2020**, *321*, 128441. [[CrossRef](#)]
61. Reed, J.; Ho, H.; Jolly, W. Chemical synthesis with a quenched flow reactor Hydroxytrihydroborate and peroxytrihydroborate. *J. Am. Chem. Soc.* **1974**, *96*, 1248–1249. [[CrossRef](#)]

Disclaimer/Publisher’s Note: The statements, opinions and data contained in all publications are solely those of the individual author(s) and contributor(s) and not of MDPI and/or the editor(s). MDPI and/or the editor(s) disclaim responsibility for any injury to people or property resulting from any ideas, methods, instructions or products referred to in the content.